Turbulent Convection over Rough Surfaces

Y. Shen and P. Tong

Department of Physics, Oklahoma State University, Stillwater, Oklahoma 74078

K.-Q. Xia

Department of Physics, The Chinese University of Hong Kong, Shatin, New Territories, Hong Kong

A light scattering experiment of turbulent convection in water is carried out in a convection cell with rough upper and lower surfaces. The vertical heat flux is found to be increased by ∼20% when the Rayleigh number becomes larger than a transition value. The experiment reveals that the main effect of the surface roughness is to increase the emission of large thermal plumes, which travel vertically through the central region. These extra thermal plumes enhance the heat transport, and they are also responsible for the anisotropic behavior of velocity fluctuations at the cell center.

PACS numbers: 47.27.Te, 05.40.+j, 42.25.–p,

Turbulent Rayleigh-Bénard convection has attracted much attention in recent years [1]. Intermittent bursts of thermal plumes from the thermal boundary layers and the coherent large-scale circulation, which modifies the boundary layers via its shear, are found to coexist in a closed convection cell [1]. These two salient features of turbulent convection are directly related to the transport of heat and momentum across the cell, and have been adopted in several theoretical models [1–3] to explain the observed scaling laws in the heat flux and temperature statistics [2,4]. The theoretical calculations arrive at similar conclusions for the temperature field, but have different assumptions and predictions for the velocity field near the boundary. Direct measurements of the velocity field under different boundary conditions, therefore, become important to determine the relative contributions of the thermal plumes and the large-scale circulation to the heat transport in turbulent convection [5–7]. In contrast to many previous convection experiments, which were conducted in a closed cell with smooth upper and lower surfaces, we report in this Letter a light scattering study of turbulent convection in a cell with rough upper and lower surfaces. Previous studies of smooth-wall and rough-wall boundary layers in wind tunnels and other open systems have shown that a comparative study of turbulence under different boundary conditions can greatly benefit our understanding of the structure of the turbulent boundary layers [8]. The study of turbulent convection over rough surfaces is also relevant to many practical applications in engineering, geography, and meteorology. An example is convection in the atmosphere and oceans, where the underlying surfaces are almost always rough.

Our experiment was conducted in a vertical cylindrical cell filled with water. Two identical cells, one has smooth upper and lower surfaces ("smooth cell") and the other has rough upper and lower surfaces ("rough cell"), were made for comparison. The smooth upper and lower plates were made of brass. The rough surfaces were made from identical brass plates but had woven V-shaped grooves on them. The grooves had a vertex angle of 90°, and their spacing was such that a square lattice of pyramids was formed on the surface. The height of the pyramids (the roughness height h) was 3.175 mm and their spacing $s = 6.35$ mm. Both the smooth and rough surfaces were electroplated with a thin layer of gold. There was a filling stem on the upper plate, and a vertical laser beam could pass through the stem and enter the central region of the cell. The sidewall of the cell was a cylindrical ring made of transparent Plexiglas to admit the incident light and transmit the scattered light. Two cylindrical rings with the same inner diameter of 20 cm but with two different heights of 20 and 40 cm were used, respectively, to extend the accessible range of the Rayleigh number. The corresponding aspect ratios ($A =$ diameter/height) are 1.0 and 0.5. The temperature of the upper plate was regulated by passing cold water through the cooling chamber fitted on the top of the plate. The lower plate was heated uniformly with an electric heating film attached to the backside of the plate. The temperature difference ΔT between the two plates was measured by two thermistors embedded in the two plates. The vertical heat flux across the cell was determined from the power required to keep the lower plate at a constant temperature. In the thermal measurements, the cell was well insulated to prevent heat leakage. The control parameter in the experiment is the Rayleigh number Ra, which is proportional to ΔT and to the cube of the cell height L.

Figure 1 compares the measured Nusselt number Nu(Ra) (the normalized heat flux) in the rough cells (open circles) with that in the smooth cells (solid triangles). The measurements were conducted in the cells with (a) $A = 0.5$ and (b) $A = 1.0$. The measured Nu(Ra) in both smooth cells is well described by the power law Nu $= 0.16$Ra$^\beta$ (solid lines). The scaling exponent $\beta = 0.281 \pm 0.015$, which agrees well with previous measurements [4,5,9]. The measured heat flux in the
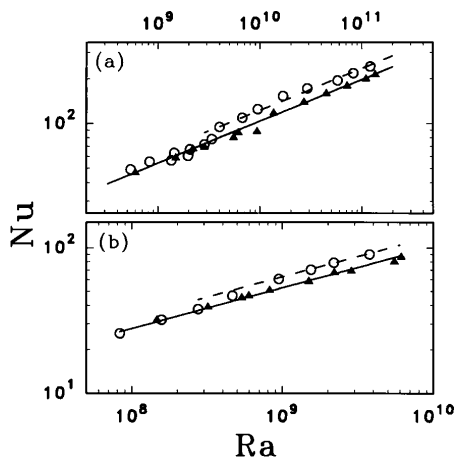
FIG. 1.   The measured Nusselt number Nu as a function of Ra in the smooth cells (solid triangles) and in the rough cells (open circles) with (a) $A = 0.5$ and (b) $A = 1.0$.   The solid lines are the power law fits $Nu = 0.16 Ra^{0.281}$ to the solid triangles, and the dashed lines indicate the power law $Nu = 0.19 Ra^{0.281}$ for the open circles.

rough cells is found to be the same as that in the smooth cells for small values of Ra.   When Ra becomes larger than a transition value Ra_0, the measured Nu is increased by ~20% as compared with that in the smooth cells.   It is seen from Fig. 1 that the onset of the enhanced heat transport occurs at $Ra_0 \simeq 4 \times 10^8$ in the $A = 1.0$ cell and at $Ra_0 \simeq 5 \times 10^9$ in the $A = 0.5$ cell.   It is notable that in the (limited) range of Ra $(>Ra_0)$ the rough-cell data can also be described by a power law with the same exponent β as that for the smooth cells, but the amplitude is changed from 0.16 to 0.19 (dashed lines).

To judge the effect of the surface roughness on the heat transport, it is necessary to compare the roughness height h with the thermal boundary layer thickness $\delta_{th}(Ra)$. When h is small compared with δ_{th}, the rough elements on the surface are buried beneath the thermal boundary layer, and hence the effect of the surface roughness will be small (low Ra region).   In the opposite limit of large Ra, where $h > \delta_{th}$, the surface roughness will strongly affect temperature fluctuations near the surface and thereby will alter the heat transport.   The values of δ_{th} can be calculated from the measured Nu using the well-tested relation $\delta_{th} = L/2Nu$ [7].   At the transition Rayleigh number Ra_0, we find $\delta_{th} \simeq 2.4$ mm for both smooth cells.   The corresponding length ratio $\delta_{th}/h \simeq 0.8$, which is close to unity.   Figure 1 thus supports the above arguments for the onset of the enhanced heat transport.

To further understand the mechanism for the enhanced heat transport in the rough cells, we measure the local velocity v and its statistics in the central region using a recently developed technique of incoherent cross-correlation spectroscopy [10].   The experimental setup and apparatus have been detailed elsewhere [10], and here we only

mention some key points.   In the experiment (to be described below) a laser beam from an argon-ion laser traverses through the convecting fluid.   The laser is under multiline operation, and the beam consists of light with a wavelength range from 457.9 to 514.5 nm.   The convecting fluid (distilled water) is seeded with neutrally buoyant polymer latex spheres (0.95 μm in diameter), which scatter light and follow the local flow.   Two photomultipliers are used to record the two strongest scattering intensities, $I_b(t)$ and $I_g(t)$, of the blue and green lights, respectively.   The velocity of the seed particles is determined by measuring the time required for the particles to cross the laser beam with a known waist radius r_0.   Experimentally, this transit time is obtained from the intensity cross-correlation function

$$g_c(t) = \frac{\langle I_b(t' + t) I_g(t') \rangle}{\langle I_b \rangle \langle I_g \rangle} = 1 + b G_c(t), \qquad (1)$$

where b (≤ 1) is an instrumental constant.   Because there is no phase coherence between $I_b(t)$ and $I_g(t)$, $g_c(t)$ is only sensitive to the scattering amplitude fluctuations produced by the seed particles moving in and out of the laser beam.

When the seed particles have a uniform velocity v in the direction perpendicular to the laser beam, $G_c(t)$ in Eq. (1) takes the form [10]

$$G_c(t) = \frac{1}{N} e^{-(vt/r_0)^2}, \qquad (2)$$

where N is the average number of the particles in the scattering volume.   To get Eq. (2) we have assumed that the laser beam has a Gaussian profile $I(r) = I_0 \exp[-2(r/r_0)^2]$, with r being the radial distance from the beam center and I_0 the light intensity at $r = 0$.   For turbulent flows $G_c(t)$ becomes

$$G_c(t) = \frac{1}{N} \int_{-\infty}^{\infty} dv_i \int_{-\infty}^{\infty} dv_j \, P_2(v_i, v_j) e^{-(v_i^2 + v_j^2)t^2/r_0^2},$$

$$(3)$$

where $P_2(v_i, v_j)$ is the probability density function (PDF) for the velocity components v_i and v_j in two different directions, both orthogonal to the incident laser beam. Because of the radial symmetry of the laser beam, $G_c(t)$ is only sensitive to $v_i^2 + v_j^2$.   This feature is particularly useful in studying the convective flow in the central region, where the mean velocity is zero [7] and thus velocity fluctuations can be directly measured.

In our experiment a lens, which was placed at 90° with respect to the incident direction, projected the scattered laser beam in the convection cell onto a slit with a 1:1 magnification.   Light passing through the slit fell on two photomultipliers (PM), which recorded the time-varying intensities $I_b(t)$ and $I_g(t)$, respectively.   The two PM's

were placed far behind the slit and mounted at a right angle on a cubic box with a beam splitter at its center. The output signals from the two PM's were fed to a digital correlator (ALV-5000), whose output gives $g_c(t)$. Each $g_c(t)$ was measured for more than 20 min to ensure that the time average has included all flow configurations. This long-time averaging is essential in order to obtain an accurate rms velocity. Because the acceptance angle of the receiving optics was large enough, small amplitude beam wandering in the convecting fluid would not affect the measurement of $g_c(t)$. The beam profile $I(r)$ was measured using a micrometer-driven translational stage, a small pinhole (5 μm in diameter), and a photodiode. It is found that the measured $I(r)$ is indeed of a Gaussian form with the beam radius $r_0 = 48 \pm 3$ μm.

Figure 2 shows the measured $G_c(t)$ in the rough cells at various values of Ra, when the laser beam was (a) horizontally and (b) vertically shone through the cell center. Note that the two beam orientations actually probe different components of the local velocity. In the former case (horizontal beam), the velocity components in the vertical direction and in one of the horizontal directions are measured, whereas in the latter case (vertical beam), only the horizontal components of the local velocity are measured. It is seen from Fig. 2(b) that the functional form of $G_c(t)$ is well described by the Lorentzian function $1/[1 + (\Gamma t)^2]$ (solid curve), and the decay rate Γ changes with Ra. Plots of $G_c(t)$ at different Ra superimpose with each other once the time axis is scaled by Γ. According to Eq. (3), the velocity PDF, $P_2(v_i, v_j)$, can be obtained by a simple Laplace inversion of the measured $G_c(t)$. For a Lorentzian $G_c(t)$, we find the corresponding $P_2(v_i, v_j)$ is of the Gaussian form

$$P_2(v_i, v_j) = \frac{1}{v_0^2} e^{-(v_i^2 + v_j^2)/v_0^2}, \tag{4}$$

where $v_0 = r_0 \Gamma$ is the rms velocity. To obtain Eq. (4), we have used the fact that velocity fluctuations in the horizontal directions are isotropic. Gaussian-like velocity PDF's have also been found in the smooth cells [11]. Figure 2(b) thus suggests that the statistics of velocity fluctuations in the horizontal directions are not strongly influenced by the surface roughness. In contrast to horizontal velocity fluctuations, however, velocity fluctuations in the vertical direction are affected by the surface roughness. As shown in Fig. 2(a), when the laser beam is horizontally shone through the cell center, the measured $G_c(t)$ changes its functional form as Ra is increased. Near the transition Rayleigh number Ra$_0$ ($\simeq 4 \times 10^8$), the decay of $G_c(t)$ is slower than a Lorentzian function. When Ra becomes much larger than Ra$_0$, $G_c(t)$ approaches the Lorentzian form (solid curve). This behavior is found in both rough cells.

To characterize the decay of a non-Lorentzian $G_c(t)$, we measure its half-decay time $T_{1/2}$. For a Lorentzian
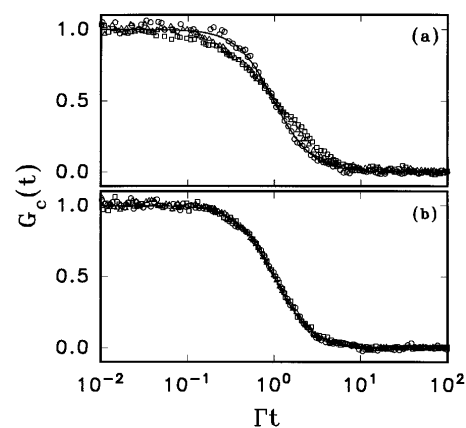

FIG. 2.   The measured $G_c(t)$ vs Γt in the rough cells when the laser beam was (a) horizontally and (b) vertically shone through the cell center. The experimental conditions are (a) Ra $= 1.2 \times 10^{10}$ (circles), 1.2×10^9 (triangles), and 3.4×10^8 (squares) all in the $A = 1.0$ cell; (b) Ra $= 4.5 \times 10^8$ (triangles), 2.5×10^9 (circles), in the $A = 1.0$ cell, and Ra $= 7.0 \times 10^{10}$ (squares) in the $A = 0.5$ cell. The solid curves are the Lorentzian function $1/[1 + (\Gamma t)^2]$.

function the half-decay time $T_{1/2} = 1/\Gamma$. With the measured r_0 and Γ (or $T_{1/2}$), we now plot the rms velocity v_0 ($= r_0 \Gamma = r_0/T_{1/2}$) as a function of Ra. Figure 3 compares the measured v_0 for the vertical beam (solid circles) with that for the horizontal beam (open squares) at different Ra. The measurements were conducted in the rough cells with (a) $A = 0.5$ and (b) $A = 1.0$. It is seen from Fig. 3 that the convective flow changes its characteristics when Ra reaches the transition Rayleigh number Ra$_0$. The values of Ra$_0$ found in Fig. 3 correspond well with those obtained from the Nu measurements in Fig. 1. When Ra is below Ra$_0$ (i.e., when $h < \delta_{\text{th}}$), velocity fluctuations in different directions have the same rms velocity, suggesting that the flow in the central region is isotropic. Our previous experiment [11] in the smooth cells has revealed that in the hard turbulence regime (Ra $> 10^8$), velocity fluctuations are isotropic and the measured v_0 (for both beam orientations) obeys the power law 2.2×10^{-5}Ra$^{0.44}$ (cm/sec) [solid line in Fig. 3(a)]. [If the Peclet number Pe ($= v_0 h/\kappa$) is chosen as a dimensionless velocity, the power law becomes Pe $= 0.30$Ra$^{0.44}$.] Figure 3(a) shows that the values of v_0 obtained in the rough cell coincide with those in the smooth cell when Ra $<$ Ra$_0$. This observation further supports our argument that when the roughness height h is smaller than the thermal boundary layer thickness δ_{th}, the flow in the rough cell should behave the same as that in the smooth cell.

When Ra becomes larger than Ra$_0$, the measured v_0 in the rough cells deviates from that in the smooth cells, and it also changes with the beam orientation. It is seen from Fig. 3 that the surface roughness affects the vertical velocity fluctuations (horizontal beam) more than the horizontal velocity fluctuations (vertical beam). The dashed lines in Fig. 3(a) are the attempted power law fits
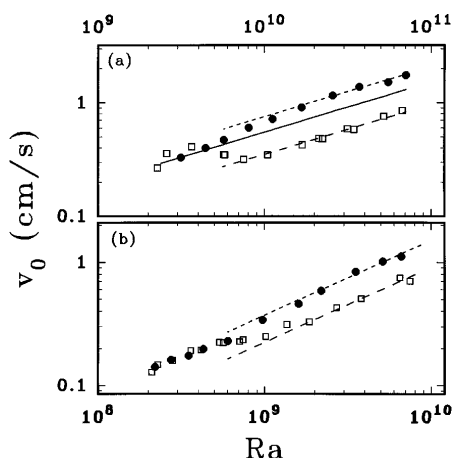
FIG. 3. The measured v_0 vs Ra for the vertical beam (solid circles) and for the horizontal beam (open squares) in the rough cells with (a) $A = 0.5$ and (b) $A = 1.0$. The solid line in (a) represents the power law $2.2 \times 10^{-5}\text{Ra}^{0.44}$ obtained in the smooth cell. The dashed lines in (a) are the attempted power law fits $1.4 \times 10^{-5}\text{Ra}^{0.44}$ (long-dashed line) and $3.0 \times 10^{-5}\text{Ra}^{0.44}$ (short-dashed line). The dashed lines in (b) are $0.73 \times 10^{-6}\text{Ra}^{0.61}$ (long-dashed line) and $1.2 \times 10^{-6}\text{Ra}^{0.61}$ (short-dashed line).

$1.4 \times 10^{-5}\text{Ra}^{0.44}$ (long-dashed line), $3.0 \times 10^{-5}\text{Ra}^{0.44}$ (short-dashed line), and those in Fig. 3(b) are $0.73 \times 10^{-6}\text{Ra}^{0.61}$ (long-dashed line) and $1.2 \times 10^{-6}\text{Ra}^{0.61}$ (short-dashed line). Note that the power law fits in Fig. 3 are different among themselves both in amplitude and in exponent. Figure 3 thus indicates that velocity fluctuations in the vertical direction parallel to gravity become substantially different from those in the horizontal directions, once the flow feels the surface roughness (i.e., when $h > \delta_{\text{th}}$). This anisotropic behavior of velocity fluctuations in the rough cells at large Ra ($> \text{Ra}_0$) is very similar to that found in the smooth cells [11] at small Ra in the soft turbulence regime, in which the thermal plumes span the full height of the cell [5]. By comparing Fig. 3 with Fig. 1, one finds that the anisotropic behavior of velocity fluctuations in the central region is directly related to the enhanced heat transport as shown in Fig. 1.

From the temperature and velocity measurements in the rough and smooth cells, we conclude that the main effect of the surface roughness is to increase the emission of large thermal plumes from the interstices between the roughness elements, and these large thermal plumes travel vertically from the boundary into the cell center. The extra thermal plumes produced by the surface roughness enhance the heat transport, and they are also responsible for the anisotropic behavior of velocity fluctuations in the central region. Similar increase in intermittent bursting of coherent structures is also found in the wind tunnel with rough walls [12,13]. Our experiment reveals that the influence of the surface roughness is not only confined to the near-wall region, but also extended into the central region of the cell. When the flow feels the surface roughness, the power law behavior of velocity fluctuations is changed considerably, even though the exponent β for the normalized heat flux Nu remains unchanged. It appears that the scaling behavior of velocity fluctuations (and temperature fluctuations) in the central region is very sensitive to the detail structure of turbulence, whereas the power law exponent β for Nu is not. The striking effects of the surface roughness reported in this Letter provide new insights into the roles of the thermal plumes played in determining the heat transport in turbulent convection. The discovery of the enhanced heat transport in the rough cells also has important applications in engineering for more efficient heat transfer.

[1] See, for example, E. Siggia, Annu. Rev. Fluid Mech. **26**, 137 (1994), and references therein.

[2] B. Castaing, G. Gunaratne, F. Heslot, L. Kadanoff, A. Libchaber, S. Thomae, X.-Z. Wu, S. Zaleski, and G. Zanetti, J. Fluid Mech. **204**, 1 (1989).

[3] B. I. Shraiman and E. D. Siggia, Phys. Rev. A **42**, 3650 (1990).

[4] F. Heslot, B. Castaing, and A. Libchaber, Phys. Rev. A **36**, 5870 (1987); X.-Z. Wu, L. Kadannoff, A. Libchaber, and M. Sano, Phys. Rev. Lett. **64**, 2140 (1990).

[5] T. H. Solomon and J. P. Gollub, Phys. Rev. Lett. **64**, 2382 (1990); Phys. Rev. A **43**, 6683 (1991); B. J. Gluckman, H. Willaime, and J. P. Gollub, Phys. Fluids **5**, 647 (1993).

[6] F. Chillá, S. Ciliberto, and C. Innocenti, Europhys. Lett. **22**, 681 (1993).

[7] A. Belmonte, A. Tilgner, and A. Libchaber, Phys. Rev. Lett. **70**, 4067 (1993); Phys. Rev. E **47**, R2253 (1993); Phys. Rev. E **50**, 269 (1994).

[8] See, for example, M. R. Raupach, R. A. Antonia, and S. Rajagopalan, Appl. Mech. Rev. **44**, 1 (1991), and references therein.

[9] H. Tanaka and H. Miyata, Int. J. Heat Mass Transfer **23**, 1273 (1980).

[10] P. Tong, K.-Q. Xia, and B. J. Ackerson, J. Chem. Phys. **98**, 9256 (1993).

[11] Y. Shen, K.-Q. Xia, and P. Tong, Phys. Rev. Lett. **75**, 437 (1995).

[12] A. J. Grass, J. Fluid Mech. **50**, 233 (1971); A. J. Grass, R. J. Stuart, and M. Mansour-Tehrani, AIAA J. **31**, 837 (1993).

[13] P.-A. Krogstad, R. A. Antonia, and L. W. B. Browne, J. Fluid Mech. **245**, 599 (1992); P.-A. Krogstad and R. A. Antonia, J. Fluid Mech. **277**, 1 (1994).